

Ping Xu · Huawu Liu

Models of microfibril elastic modulus parallel to the cell axis

Received: 4 November 2002 / Published online: 8 May 2004
© Springer-Verlag 2004

Abstract Based on different physical assumptions six possible models are developed or adopted concerning the component of the elastic modulus of a single microfibril, i.e. the elastic modulus that is parallel to cell axis about which the microfibril is coiled like a loose or lazy spring. A thorough evaluation regarding the disparities between the rigorous and simplified models is presented. The simulation demonstrates that the simplified models differ considerably from the rigorous one especially in the small microfibril angle range. This would explain the poor estimations of cell wall stiffness at low microfibril angles as seen in previous modelling studies.

Introduction

Most of previous theoretical studies focused on the cell wall, and there has been an absence of a thorough study regarding the mechanical properties of single wood microfibril. The wood cell wall consists of cellulose microfibrils embedded in a lignin-hemicelluloses matrix with the microfibrils coiled in a helix-like path within the cell wall (Yamamoto and Kojima 2002). This means that: (1) microfibrils are crucial to the mechanical properties of the cell wall; (2) a single microfibril is more flexible where a load is applied parallel to the cell axis than where the same load is applied parallel to the microfibril itself, in a similar way as a spring reacts to external forces; (3) an increase in the microfibril angle would reduce the contribution of the microfibril to the cell wall stiffness and so lead to a poor wood quality.

Hearle (1963) first attempted to quantify the structural effect of a helical microfibril on the stiffness of plant cells (Preston 1974). Later Preston (1974) and his co-workers adopted Hearle's model to account for the reduction of wood cell stiffness due to microfibril angle. The first model assumed the microfibril was an isotropic material whereas Cowdrey and Preston in 1966 proposed a second model for an "anisotropic homogeneous wall" (cited in Preston 1974). Cave (1968) suggested that

P. Xu (✉) · H. Liu
Forest Research, Forestry Road, University of Canterbury,
PO Box 29 237, Fendalton, Christchurch, New Zealand
E-mail: ping.xu@forestresearch.co.nz

...the uniform distribution of the crystal planes parallel to the microfibril axis makes the cellulose appear isotropic in the plane normal to the microfibril axis and allows the mathematical representation of the cellulose to be simplified to an equivalent fibre with transverse isotropic elastic properties equal to the average in plane normal to the microfibril axis.

Thus, the cell wall was assumed as a planar mat of transversely isotropic microfibrils embedded in a homogenous and isotropic matrix, and a cell wall was divided into a series of elementary slabs with all microfibrils inclined at the same angle to the cell axis within a slab (Cave 1968). Cave (1968) proposed a formula to convert the elastic constants of microfibrils to the cell coordinate system, which may be treated as the third model for the elastic modulus parallel to the cell axis (Cave 1968, 1969; Cave and Walker 1994). Later, Yamamoto and Kojima (2002) introduced the fourth model for their study concerning single cell shrinkage, which is mathematically a further simplification of Cave's model.

Cave's material model of microfibrils and his estimation of cell wall stiffness have been frequently quoted (Cave 1976, 1978; Cave and Walker 1994; Astley et al. 1998). However, the predicted cell wall stiffness arising from Cave's microfibril elasticity model showed a considerable disparity with his experimental results at lower microfibril angles (Fig. 1). Comparing the experimental

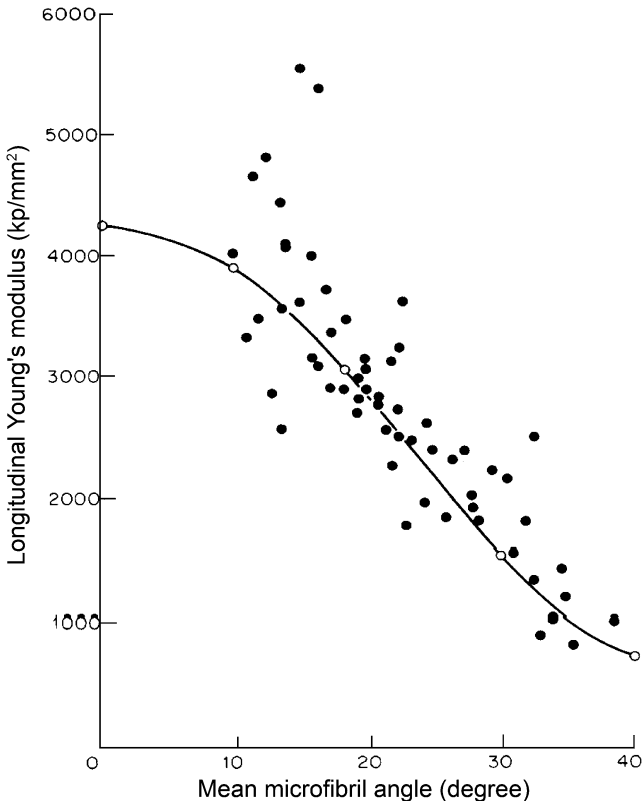


Fig. 1 The predictions and measurements of cell wall stiffness vs. mean microfibril angle (after Cave 1968). Note: —○— represents the theoretical curve; • represents the experimental data

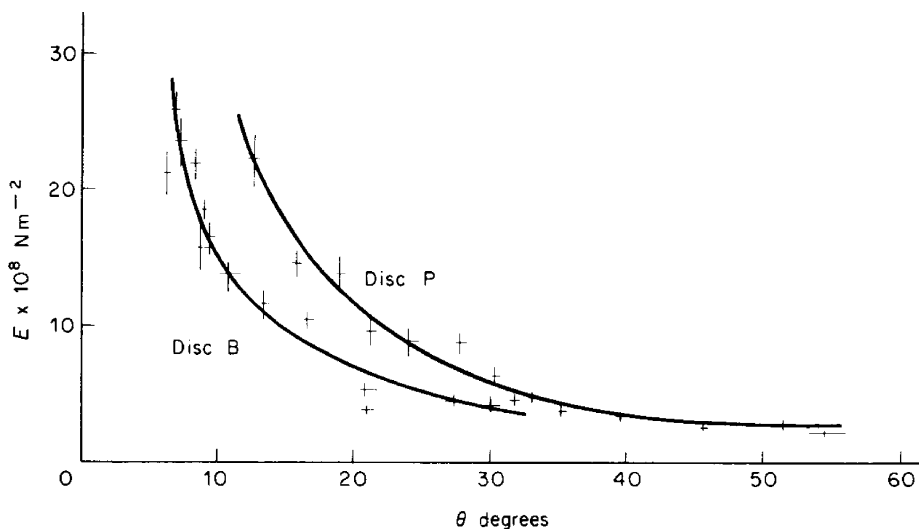


Fig. 2 The experimental relationships between stiffness and mean microfibril angle in S2 layer of *Picea* wood cell (after Preston 1974). Note: — represents the experimental curve; + represents the experimental data

curve (Fig. 2) with Cave's theoretical curve (Fig. 1), one can see the experimental curve behaved completely different from the theoretical curve: the experimental curve is concave in form whereas the theoretical prediction is sigmoidal. Similar problems existed when applying those previous models to the estimation of cell wall stiffness in other tree species and in other plants (Hearle 1963; Navi 1998). These disagreements at low microfibril angles necessitate a thorough investigation on the mechanical models for the modulus component parallel to the cell axis in the microfibril compliance and stiffness matrices as well as the errors arising from the simplified models. This paper aims to examine the basis for calculation of the elastic modulus parallel to the cell axis in single microfibril to provide a solid base for succeeding studies of cell wall stiffness.

Features of a single microfibril

Microfibrils are known to be pure crystalline cellulose I consisting of two distinct forms of molecular packing, i.e. cellulose I_α (triclinic) and cellulose I_β (monoclinic). Wada et al. (1994) reported that cellulose I_β was a major sub-allomorph of wood cellulose, while a test using carbon-13 nuclear magnetic resonance showed that cellulose I_α and I_β were present in almost equal parts in *Pinus radiata* (the fraction of I_α was 0.51) (Newman 1999). Brown (1999) reported that "Usually these two sub-allomorphs coexist together within a given microfibril". However, the precise manner in which I_β and I_α are distributed in wood microfibril is still not well-known.

The cellulose microfibrils have been assumed transverse isotropy in the early studies (Cave 1968, 1969, 1976; Mark 1967; Bodig and Goodman 1973; Preston 1974). Recently, it has been found that the cellulose chains were less tightly-packed on the surface than they were within the microfibril (Kroon-Batenbury

et al. 1986; Newman 1994, 1998, 1999). This means that a wood microfibril is actually a composite with a highly ordered core and a surface layer in which the cellulose chains are only hydrogen-bonded to the interior chains on only one side (Tashiro and Kobayashi 1991; Reiling and Brickmann 1995). Thus the elastic constants of a microfibril should be the weighted-average of the constituents over their volume fractions, following the rule of mixtures. Unfortunately, there is not enough direct data allowing one to derive the stiffness matrix of the cellulose chains lying in the surface layer of the microfibril. Only one of the elastic constants, i.e. the longitudinal elastic modulus of single microfibril, was estimated recently using an indirect method (Newman 1998, 1999). Therefore, this paper uses the microfibril stiffness matrix data from the earlier literature (Mark 1965, 1967). This should not affect our comments about the difference observed when comparing models of varying rigour.

The cross-section of microfibrils has been proposed as square, rectangular or hexagonal in different publications (Preston 1974; Fengel and Wegener 1984; Sugiyama et al. 1986; Newman 1998). The size of microfibril in *Pinus* species has decreased as the resolving power of electron microscopy improved, from a mean width of 3.5 nm (Heyn 1969) to 2.5 nm (Harada and Goto 1982). Following the descriptions of microfibril geometry, this paper assumes a slim prismatic microfibril with uniform cross-section and constant spatial angle θ between the microfibril path and the cell axis.

The rigorous model

In modelling, a cell wall can be “opened” into a flat sheet with orthotropic or transverse isotropic microfibrils embedded in an isotropic matrix. To apply Hooke’s Law of angle lamina (Jones 1975), a global coordinate system (x_1, x_2, x_3) is used for the cell and a local coordinate system (l, r, t) for the microfibril, where (x_1, x_2, x_3) and (l, r, t) stand for longitudinal, radial and tangential directions in the cell and the microfibril coordinate system, respectively. Microfibril angle is denoted by the angle θ between l and x_1 (Fig. 3).

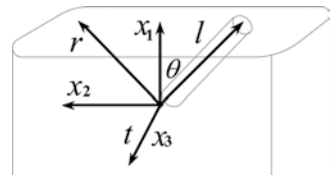
Define $\{\epsilon_f\}^T = \{\epsilon_l, \epsilon_r, \epsilon_t, \gamma_{rt}, \gamma_{tl}, \gamma_{lr}\}$ and $\{\sigma_f\}^T = \{\sigma_l, \sigma_r, \sigma_t, \tau_{rt}, \tau_{tl}, \tau_{lr}\}$ as the strain and stress tensors in the local coordinate system of the microfibril; and $\{\epsilon_c\}^T = \{\epsilon_1, \epsilon_2, \epsilon_3, \gamma_{23}, \gamma_{31}, \gamma_{12}\}$ and $\{\sigma_c\}^T = \{\sigma_1, \sigma_2, \sigma_3, \tau_{23}, \tau_{31}, \tau_{12}\}$ as the strain and stress tensors in the global coordinate system of the wood cell, respectively. In these vectors, the subscripts f and c indicate the microfibril and the cell correspondingly. The transformation relationships of strain and stress are:

$$\{\epsilon_f\} = [R][T][R]^{-1}\{\epsilon_c\} \tag{1}$$

and

$$\{\sigma_f\} = [T]\{\sigma_c\} \tag{2}$$

Fig. 3 Coordinate systems of the cell and the microfibril (θ is the microfibril angle)



where $[R]$ is the Reuter matrix, $[T]$ is the transformation matrix, $[R]^{-1}$ is the inverse of $[R]$, $[T]^T$ is the transpose of $[T]$ and

$$[T] = \begin{bmatrix} c^2 & s^2 & 0 & 0 & 0 & 2sc \\ s^2 & c^2 & 0 & 0 & 0 & -2sc \\ 0 & 0 & 1 & 0 & 0 & 0 \\ 0 & 0 & 0 & c & -s & 0 \\ 0 & 0 & 0 & s & c & 0 \\ -sc & sc & 0 & 0 & 0 & c^2 - s^2 \end{bmatrix} \quad c = \cos(-\theta), s = \sin(-\theta) \quad (3)$$

$$[R] = \begin{bmatrix} 1 & 0 & 0 & 0 & 0 & 0 \\ 0 & 1 & 0 & 0 & 0 & 0 \\ 0 & 0 & 1 & 0 & 0 & 0 \\ 0 & 0 & 0 & 2 & 0 & 0 \\ 0 & 0 & 0 & 0 & 2 & 0 \\ 0 & 0 & 0 & 0 & 0 & 2 \end{bmatrix} \quad (4)$$

Denote $[S] = [S_{ij}]$ and $[\bar{S}](i, j = 1, 2, \dots, 6)$ as the compliance matrices of the microfibril in the local and global coordinate systems, respectively; $[C] = [S]^{-1}$ and $[\bar{C}] = [\bar{S}]^{-1}(i, j = 1, 2, \dots, 6)$ as the corresponding stiffness matrices. For an orthotropic material, there are twelve elastic constants (nine independent) in the symmetric compliance matrix, and these are described as elastic moduli (E_l, E_r, E_t), shear moduli (G_{rt}, G_{lt}, G_{lr}) and Poisson's ratios ($\nu_{lr}, \nu_{rt}, \nu_{lt}, \nu_{lt}, \nu_{rt}, \nu_{lr}$). For an orthotropic material,

$$[S_{ij}] = \begin{bmatrix} 1/E_l & -\nu_{lr}/E_l & -\nu_{lt}/E_l & 0 & 0 & 0 \\ -\nu_{rl}/E_r & 1/E_r & -\nu_{rt}/E_r & 0 & 0 & 0 \\ -\nu_{tl}/E_t & -\nu_{tr}/E_t & 1/E_t & 0 & 0 & 0 \\ 0 & 0 & 0 & 1/G_{rt} & 0 & 0 \\ 0 & 0 & 0 & 0 & 1/G_{lt} & 0 \\ 0 & 0 & 0 & 0 & 0 & 1/G_{lr} \end{bmatrix} \quad (5)$$

Note that transverse isotropy is a specific case of orthotropy with $S_{11} = S_{22}, S_{13} = S_{12}, S_{44} = 2(S_{22} - S_{23})$ and $S_{66} = S_{55}$ (Jones 1975).

The stress-strain relationships of the microfibril in the local system are

$$\{\varepsilon_f\} = [S]\{\sigma_f\} \quad (6)$$

and

$$\{\sigma_f\} = [C]\{\varepsilon_f\} \quad (7)$$

Substituting Eqs. 1 and 2 into 6 and 7, the stress-strain relationships of the microfibril in the global system are given by

$$\{\varepsilon_c\} = [R][T]^{-1}[R]^{-1}[S][T]\{\sigma_c\} = [T]^T[S][T]\{\sigma_c\} = [\bar{S}]\{\sigma_c\} \quad (8)$$

$$\{\sigma_c\} = [T]^{-1}[C][R][T][R]^{-1}\{\varepsilon_c\} = [T]^{-1}[C][T^{-1}]^T\{\varepsilon_c\} = [\bar{C}]\{\varepsilon_c\} \quad (9)$$

Under uniaxial loading on the wood cell, we have the stress tensor $\{\sigma_{c1}\} = \{\sigma_1, 0, 0, 0, 0, 0\}^T$. Substituting this condition to Eq. 8 yields

$$\begin{aligned} [\bar{S}]\{\sigma_{c1}\} &= \sigma_1 \{\bar{S}_{11}, \bar{S}_{12}, \bar{S}_{13}, 0, 0, \bar{S}_{16}\}^T \\ &= \{\varepsilon_{c1}\} = \frac{\varepsilon_1}{\bar{S}_{11}} \{\bar{S}_{11}, \bar{S}_{12}, \bar{S}_{13}, 0, 0, \bar{S}_{16}\}^T \end{aligned} \quad (10)$$

$$\varepsilon_1 = \bar{S}_{11}\sigma_1 \quad (11)$$

Note that $[\bar{S}]$ and $[\bar{C}]$ are mutually inverse and $\sum C_{1j}S_{j1} = 1$. Eq. 11 can also be obtained by multiplying Eq. 10 by $[\bar{C}]$ on both sides, which gives

$$[\bar{C}]\{\varepsilon_{c1}\} = [\bar{C}][\bar{S}]\{\sigma_{c1}\} = \sigma_{c1} \quad (12)$$

$$\sigma_1 = \frac{\varepsilon_1}{\bar{S}_{11}} \sum C_{1j}S_{j1} = \frac{\varepsilon_1}{\bar{S}_{11}} \quad (13)$$

Therefore, the elastic modulus parallel to the cell axis in single microfibril (i.e. the contribution of single microfibril to the longitudinal stiffness of the cell) can be rigorously expressed as

Model 1

$$\begin{aligned} \bar{E}_f(\theta) &= (\bar{S}_{11})^{-1} = [S_{11}\cos^4\theta + (2S_{12} + S_{66})\sin^2\theta\cos^2\theta + S_{22}\sin^4\theta]^{-1} \\ &= \left[\frac{\cos^4\theta}{E_l} + \left(\frac{-2\nu_{lr}}{E_l} + \frac{1}{G_{lr}} \right) \sin^2\theta\cos^2\theta + \frac{\sin^4\theta}{E_r} \right]^{-1} \end{aligned} \quad (14)$$

where E_l is the longitudinal elastic modulus, G_{lr} is the longitudinal-radial shear modulus, E_r is the transverse modulus of a single microfibril, ν_{lr} is the longitudinal-radial Poisson's ratio of the microfibril and θ is the microfibril angle.

Simplified models based on Hooke's Law of angle lamina

A uniaxial loading on the cell wall results in longitudinal, transverse, and longitudinal-transverse shear strains of microfibril in the global coordinate system (Eq. 10). Ignoring the transverse and shear strains and forcing the true strain tensor $\{\varepsilon_{c1}\}$ in Eq. 10 to be $\{\varepsilon_{c2}\} = \{\varepsilon_1, 0, 0, 0, 0, 0\}^T$, we have

$$\begin{aligned} [\bar{C}]\{\varepsilon_{c2}\} &= \{\sigma_{c2}\} \\ &= \varepsilon_1 \{\bar{C}_{11}, \bar{C}_{12}, \bar{C}_{13}, 0, 0, \bar{C}_{16}\}^T \end{aligned} \quad (15)$$

$$\sigma_1 = \varepsilon_1 \bar{C}_{11} \quad (16)$$

Model 2

$$\begin{aligned} \bar{E}_f(\theta) &\approx \bar{C}_{11} \\ &= C_{11} \cos^4 \theta + 2(C_{12} + 2C_{66}) \sin^2 \theta \cos^2 \theta + C_{22} \sin^4 \theta \end{aligned} \quad (17)$$

Note that Eq. 17 is the same as the model proposed by Cave (1968, 1969; Cave and Walker 1994) in terms of mechanics, but the subscripts “1, 3, 4” in Cave’s publications are denoted by “2, 1, 6” in this study due to the use of a different coordinate system. When assigning the mean microfibril angle to all microfibrils and ignoring the effect of the matrix, Eq. 17 can be considered as the cell wall stiffness, and the curve of the prediction is shaped the same as Cave’s theoretical curve shown in Fig. 1.

Substituting $\{\epsilon_{c2}\} = \{\epsilon_1, 0, 0, 0, 0, 0\}^T$ into Eq. 1, the global axial strain $\{\epsilon_{c2}\}$ of the microfibril is transformed to $\{\epsilon_{f2}\} = \epsilon_1 \{c^2, s^2, 0, 0, 0, -2sc\}^T$ in the local coordinate system. Ignoring the transverse and shear strains of the microfibril in the local coordinate system returns $\{\epsilon_{f3}\} = \epsilon_1 \{c^2, 0, 0, 0, 0, 0\}^T$ and corresponding stress

$$\{\sigma_{f3}\} = [C] \{\epsilon_{f3}\} = \varepsilon_1 \{C_{11}c^2, C_{12}c^2, C_{13}c^2, 0, 0, 0\}^T \quad (18)$$

Substituting Eq. 18 into Eq. 2, we have

Model 3

$$\bar{E}_f(\theta) = C_{11}c^4 + C_{12}c^2s^2 \quad (19)$$

Since the ratio $C_{11}:C_{12}$ is between 60:1 and 355:1 (Mark 1967), Model 3 may be further simplified to the form:

Model 4

$$\bar{E}_f(\theta) = C_{11}c^4 \quad (20)$$

Simplified models on the basis of isotropic material assumption

Allowing one turn of a microfibril on a plane would result in a right-angled triangle. Suppose that l is the length of the microfibril, h is the height of the corresponding cell portion and c is the circumference of the surface in which the microfibril lies (Fig. 4).

Thus:

$$l^2 = h^2 + c^2 \quad (21)$$

Differentiating Eq. 21 yields

$$ldl = hdh + cdc \quad (22)$$

Note that $hdh = hdh \frac{h}{h} = h^2 (dh/h)$ and $cdc = cdc \frac{c}{c} = c^2 (dc/c)$. Dividing Eq. 22 by l^2 gives

$$\frac{dl}{l} = \frac{h^2}{l^2} (dh/h) + \frac{c^2}{l^2} (dc/c) \tag{23}$$

With uniaxial force applied to the cell, the lamella has an axial strain $\epsilon_1 = d h/h$ and transverse strain dc/c for polygon-shaped cross-sections. From the definition of Poisson's ratio, we have $\nu_{12} = -(dc/c)/(dh/h)$ in the global coordinate system. In addition, $h/l = \cos\theta$, $c/l = \sin\theta$ (Fig. 4). Hence the axial strain of microfibril $\epsilon_l = d l/l$ can be expressed by

$$\epsilon_l = \epsilon_1 (\cos^2 \theta - \nu_{12} \sin^2 \theta) \tag{24}$$

Denoting the cross-section area normal to the microfibril axis as A_l and the axial elastic modulus of microfibril as E_l , the force component parallel to the cell axis is given by:

$$A_l E_l \epsilon_l \cos\theta \tag{25}$$

The cross-section of the microfibril perpendicular to the cell axis (Fig. 5) is:

$$A_f / \cos\theta \tag{26}$$

Dividing Eq. 25 by Eq. 26, the microfibril stress parallel to the cell axis becomes

Fig. 4 Geometrical relation with a single turn of a microfibril developed on the plane (θ : microfibril angle, l : microfibril length in one turn, c : circumference of the cell wall in which the microfibril lies, h : height of one turn of a microfibril)

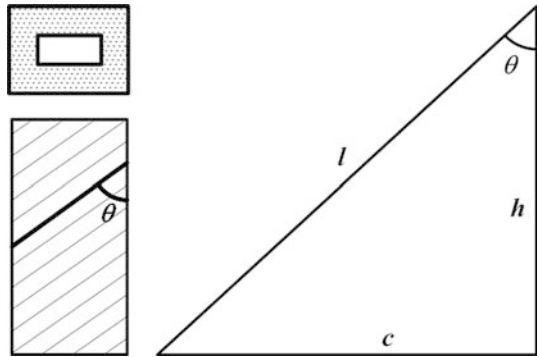
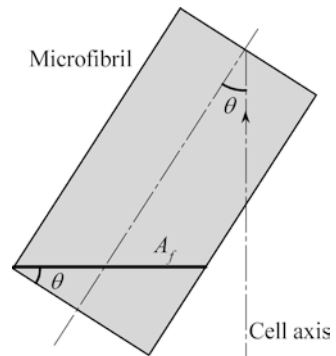


Fig. 5 Illustration of microfibril cross-section perpendicular to the cell axis



$$E_l \epsilon_l \cos^2 \theta = E_l \epsilon_1 (\cos^2 \theta - \nu_{12} \sin^2 \theta) \cos^2 \theta \quad (27)$$

Note that ϵ_1 is the microfibril strain in the cell axis direction, assuming no slippage between the microfibril and the embedding matrix. The microfibril modulus parallel to the cell axis, as the quotient of the stress over the strain, has the form

Model 5

$$\bar{E}_f[\theta] = E_l (\cos^2 \theta - \nu_{12} \sin^2 \theta) \cos^2 \theta \quad (28)$$

The cell deformation under uniaxial loading causes not only the longitudinal strain, but also the transverse and shear strain of the microfibril in the local system. Eq. 28 ignores the local lateral and shear strains of the microfibrils for two reasons: the transverse and shear moduli are negligible compared with E_l (Mark 1965, 1967); and the local lateral and shear stresses offset each other in the cell axis direction.

Further ignoring the global lateral contraction, a rough estimation of the microfibril modulus parallel to cell axis is expressed by

Model 6

$$\bar{E}_f[\theta] = E_l \cos^4 \theta \quad (29)$$

Simulations

The longitudinal elastic modulus of microfibril varies considerably from 56.5 to 246.4 GPa and the elastic to shear moduli ratios range from 6:1 to 1400:1, while the longitudinal to transverse modulus ratios are on the order of about 10:1 (Mark 1965, 1967). A set of elastic constants of microfibrils quoted from Mark (1965) by Cave (1969) are listed in Table 1.

The estimated S_{23} is negligible compared with other constants in the microfibril compliance matrix (Mark 1965, 1967). Hence, following Cave (1968,

Table 1 Constants of compliance matrix of microfibrils (after Cave 1969)

Longitudinal elastic modulus	$E_l = 137$ GPa	Mark (1965)
Transverse elastic modulus	$E_r = 15.7$ GPa	Mark (1965)
Longitudinal-transverse Poisson's ratio	$\nu_{lr} = 0.1$	Mark (1965)
Longitudinal-transverse rigidity	$G_{lr} = 3.8$ GPa	Mark (1965)
Longitudinal-transverse Poisson's ratio (of cell wall)	$*\nu_{12} = 0.2$	Estimate based on Cave (1968, 1969)

*The longitudinal-transverse Poisson's ratio of wood matrix was 0.3 and the longitudinal-transverse Poisson's ratio of the microfibrils was 0.1 (Cave 1969), while the volume ratio of the cellulose-matrix was 50:50 (Cave 1968). Thus the longitudinal-transverse Poisson's ratio of cell wall should be the weighted-average of the constituents over their volume fractions, i.e. $\nu_{12} = 0.2$.

1969) by setting $S_{23}=0$, the microfibril stiffness matrix thus can be computed from Table 1 as:

$$[C] = \begin{bmatrix} 137.315 & 1.574 & 1.574 & 0 & 0 & 0 \\ 1.574 & 15.718 & 0.018 & 0 & 0 & 0 \\ 1.574 & 0.018 & 15.718 & 0 & 0 & 0 \\ 0 & 0 & 0 & 7.85 & 0 & 0 \\ 0 & 0 & 0 & 0 & 3.8 & 0 \\ 0 & 0 & 0 & 0 & 0 & 3.8 \end{bmatrix} \quad (30)$$

Note that the calculated constants of the stiffness matrix in Eq. 30 are slightly different from Cave’s computation in which $C_{11} = 137.3$, $C_{12} = 1.572$, $C_{23} = C_{32} = 0.012$ (Cave 1969). The increase of computing power in the last years has allowed a more accurate calculation of inverse matrices using mathematical software.

Summary and discussions

Applying a uniaxial load to the cell wall, Model 1 was directly derived on the basis of Hooke’s Law of angle lamina from the compliance matrix in the global (cell) coordinate system. The uniaxial load produces a strain tensor in the microfibril, which comprises longitudinal tensile, transverse compression and longitudinal-transverse shear strains in the cell coordinate system. By ignoring the transverse and longitudinal-transverse shear strains, Model 2 was obtained from multiplying the simplified strain tensor with the stiffness matrix of the microfibril in the cell coordinate system. Further neglecting the local microfibril

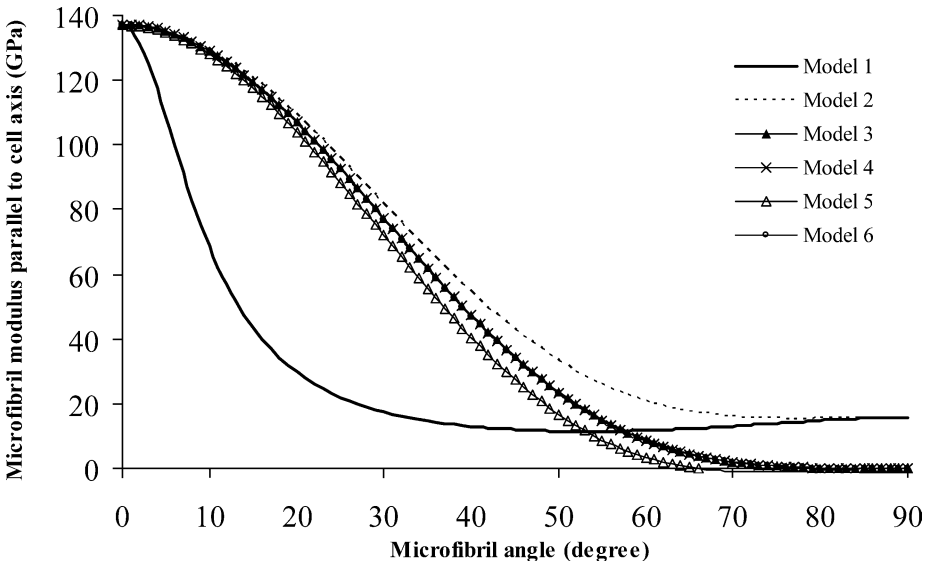


Fig. 6 Simulation for the illustration of relative model predictions. Model 1 is the rigorous model and the others are simplified models. The curves for Models 3, 4 and 6 coincide

lateral and shear strain (i.e. the transverse strain and longitudinal-transverse shear strains in the microfibril coordinate system) and the stiffness constant C_{12} , Model 3 and Model 4 were formulated. Model 5 was developed under the assumption of material isotropy and ignoring the local microfibril lateral and shear strains. The simplest of these, Model 6 was obtained by additional simplification neglecting the cell lateral contraction from Model 5.

The bias of the frequently used Model 2 arises from ignoring the global microfibril lateral and shear strains (i.e. the microfibril transverse and longitudinal-transverse shear strains in the cell coordinate system). For example, where the microfibril angle is 45° , the uniaxial loading $\{\sigma_1, 0, 0, 0, 0, 0\}^T$ on the wood cell results in a global microfibril strain tensor $\epsilon_1 \{1, -0.578, -4.398 \times 10^{-3}, 0, 0, 0.867\}^T$, which can be obtained from Eq. 10 and Table 1. Obviously, the components two and six in the strain tensor cannot be neglected compared with component one (i.e. longitudinal strain parallel to the cell axis).

Generally, model calibration allows the model user to justify the accuracy to an acceptable level, when the prediction shows a similar trend to the experimental curve. Assigning all microfibrils the same angle in S2 layer and ignoring the contribution of the matrix, the plotting in Fig. 6 may be viewed as a rough estimation of the cell wall stiffness. Obviously, Model 1 shows a similar concave trend to the experimental results shown in Fig. 1 and the experimental curve shown in Fig. 2, whereas the simplified models present sigmoidal shapes. This means the errors arising from the simplified models cannot be eliminated using calibration techniques. Hence, this paper first recommends the rigorous model for succeeding studies concerning the prediction of cell wall stiffness.

Acknowledgements The support of the AGMARDT (Agricultural and Marketing Research and Development Trust) Fund is gratefully acknowledged.

References

- Astley RJ, Stol KA, Harrington JJ (1998) Modelling the elastic properties of softwood, Part II: The cellular microstructure. *Holz als Roh- und Werkstoff* 56:43–50
- Bodig J, Goodman JR (1973) Prediction of elastic parameters for wood. *Wood Sci* 5(4):249–264
- Brown RM (1999) Cellulose structure and biosynthesis. *Pure Appl Chem* 71(5):767–775
- Cave ID (1968) The anisotropic elasticity in the plant cell wall. *Wood Sci Tech* 2:268–278
- Cave ID (1969) The longitudinal elastic modulus of *Pinus radiata*. *Wood Sci Tech* 3:40–48
- Cave ID (1976) Modelling the structure of the softwood cell wall for computation of mechanical properties. *Wood Sci Technol* 10:19–28
- Cave ID (1978) Modelling moisture-related mechanical properties of wood, Part 1: Properties of the wood constituents. *Wood Sci Technol* 12:75–86
- Cave ID, Walker JCF (1994) Stiffness of wood in fast-grown plantation softwoods: The influence of microfibril angle. *Forest Prod J* 44(5):43–48
- Fengel D, Wegener G (1984) *Wood: chemistry ultrastructure, reactions*. Walter de Gruyter, Berlin
- Harada H, Goto T (1982) The structure of cellulose microfibrils in Valonia. In: Brown RM (ed) *Cellulose and other natural polymer systems: Biogenesis, structure and degradation*. Plenum Press, New York, pp 383–401
- Hearle JWS (1963) The fine structure of fibres and crystalline polymers, Part III: Interpretation of the mechanical properties of fibres. *J Appl Polymer Sci* 7:1207–1223
- Heyn ANJ (1969) The elementary fibril and supermolecular structure of cellulose in soft wood fiber. *J Ultrastructural Res* 26:52–68
- Jones RM (1975) *Mechanics of composite materials*. Scripta Book Company, USA
- Kroon-Batenburg LMJ, Kroon J, Northolt MG (1986) Chain modulus and intramolecular hydrogen bonding in native and regenerated cellulose fibres. *Polymer Commun* 27:290–292

- Mark RE (1967) Cell wall mechanics of tracheids. Yale University Press, New Haven
- Mark RE (1965) Tensile stress analysis of the cell walls of coniferous tracheids. In: Côté WA (ed) Cellular ultrastructure of woody plants. Syracuse University Press, NY
- Navi P (1998) The influence of microfibril angle on wood cell and wood mechanical properties, experimental and numerical study. In: Butterfield BG (ed) Proc IAWA/IUFRO International Workshop on Microfibril Angle in Wood 62–70. University of Canterbury
- Newman RH (1994) Crystalline forms of cellulose in softwoods and hardwoods. *J Wood Chem Technol* 14:451–446
- Newman RH (1998) How stiff is an individual cellulose microfibril? In: Butterfield BG (ed) Proc IAWA/IUFRO International Workshop on Microfibril Angle in Wood 81–93. University of Canterbury
- Newman RH (1999) Estimation of the relative proportions of cellulose I_α and I_β in wood by carbon-13 NMR spectroscopy. *Holzforschung* 53:335–340
- Preston RD (1974) The physical biology of plant walls. Chapman and Hall, London
- Reiling S, Brickmann J (1995) Theoretical investigations on the structure and physical properties of cellulose. *Macromolecular Theory Simul* 4:725–743
- Sugiyama J, Otsuka Y, Murase H, Harada H (1986) Toward direct imaging of cellulose microfibrils in wood. *Holzforschung* 40(supplement):31–36
- Tashiro K, Kobayashi M (1991) Theoretical evaluation of three-dimensional elastic constants of native and regenerated cellulose: Role of hydrogen bonds. *Polymer J* 32(8):1516–1526
- Wada M, Sugiyama J, Okano T (1994) The monoclinic phase is dominant in wood cellulose. *Mokuzai Gakkaishi* 40(1):50–56
- Yamamoto H, Kojima Y (2002) Properties of cell wall constituents in relation to longitudinal elasticity of wood, Part I: Formulation of the longitudinal elasticity of an isolated wood fiber. *Wood Sci Technol* 36:55–74